Articles

Synergistic Effect on the Photocatalytic Degradation of 2-Chlorophenol Using TiO_2 Thin Films Doped with Some Transition Metals in Water

Oh-Jin Jung

Division of Environmental Engineering, Chosun University, Gwang-Ju 501-759, Korea
Received March 21, 2001

The metallorganic chemical vapor deposition (MOCVD) method has been used to prepare TiO_2 thin films for the degradation of hazardous organic compounds, such as 2-chlorophenol (2-CP). The effect of supporting materials and metal doping on the photocatalytic activity of TiO_2 thin films also has been studied. TiO_2 thin films were coated onto various supporting materials, including stainless steel cloth(SS), quartz glass tube (QGT), and silica gel (SG). Transition metals, such as Pd(II), Pt(IV), Nd(III) and Fe(III), were doped onto TiO_2 thin film. The results indicate that Nd(III) doping improves the photodegradation of 2-CP. Among all supporting materials studied, SS(37 μm) appears to be the best support. An optimal amount of doping material at 1.0 percent (w/w) of TiO_2-substrate thin film gives the best photodegration of 2-CP.

Keywords : Metallorganic chemical vaper deposition, Dopant TiO_2 thin film, Photocatalytic degradation.

Introduction

Photocatalysis employing wide band-gap semiconducting metal oxide (SMO) has been shown to be an effective remedy for undesired chemicals in aqueous solution.[1-4] In particular, photocatalysis with TiO_2/UV (ultraviolet) has been studied extensively.[2,5-6] Part of the attractiveness of TiO_2 in this case is due to its chemical stability, low cost and non-toxicity. However, the major impediment to its wide-spread application, particularly indoors, is the fact that it absorbs near-UV light (Eg = 3.2 eV for anatase). This band gap does not match very well with solar light. Several methods have been proposed to increase near-UV visible light absorption in TiO_2, including doping with Fe(III), Pt(IV) or other transition metals (TM).[7-9] With the presence of an electron acceptor, such as oxygen or a transition metal,[10] the recombination of electron/hole pairs can be lessen and the photocatalytic efficiency will be increased.

Photocatalytic degradation of several organic contaminants, using large band gap thin film particles, has been studied extensively.[11-13] In a slurry-based photocatalytic reactor system, the rate-determining step in the degradation process is considered to be the reduction of oxygen by trapped electrons on the thin film surface, which produces reduced oxygen species, such as the superoxide radical ions. Also, the photogenerated electron-hole pairs can recombine. Therefore, suppressing the recombination of hole-electron pairs and prolonging the life time of carriers are essential for improving the efficiency of net charge transfer at the thin film/electrolyte interface. Previous work combined two different thin films that have different band-gaps to improve the separation efficiency of carriers. These systems include Pt(IV)/TiO_2, ZnO/TiO_2 and SnO_2/TiO_2.[14-18] As for metal ion doped TiO_2 powder, transition metal ions doped TiO_2 coated on various supporters, such as powder, quartz glass and silica-gel,[19-20] were studied extensively in relation to the enhancement of the photodegradation of organic pollutants. This has been studied extensively in thin film form and synthesized by a number of methods, such as reactive sputtering,[21] plasma enhanced chemical vapor deposition,[22] low pressure chemical deposition, and metallorganic chemical vapor deposition.[23]

However, in spite of so many efforts, it is still unclear which methods and supports are the most convenient in terms of mechanical stability and photocatalytic effect.

CVD (Chemical Vapor Deposition), MOCVD, and thermal pyrolysis have been used in which molecular precussors are allowed to react at high temperatures in the gas phase or as molecular solids.

The aim of the present study is to investigate the photocatalytic behavior of some transition metals doped on the surface of supported TiO_2 catalysts prepared by the MOCVD method.

Wet chemical methods and nanostructuring titania preparation[24] were used for the synthesis of TiO_2 and TiO_2 thin films doped with some transition metals, and 2-chlorophenol (2-CP) was photodecomposed, using the thin films under air cooling and air saturation for both batch and continuous flow systems. The photocatalytic efficiencies for these thin films coated on the surface of various kinds of supports, such as stainless steel cloth (SS), quartz glass tube (QGT), and silica gel (SG), were also investigated and compared with those of TiO_2 powder.

*To whom correspondence should be addressed. Tel: +82-62-230-6644; e-mail: ojjung@mail.chosun.ac.kr

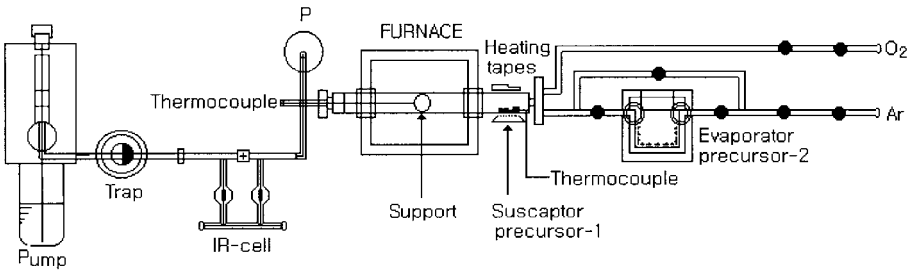

Figure 1. Hot wall low pressure MOCVD reactor: experimental setup.

Experimental Section

Materials. TiO_2(P25) and Type 304 stainless steel cloth (SS, 37 μm, $4\pi \times 10$ cm^3) were supplied by Degussa Co., Ridgefield Park, NJ., and MSC industrial supply Co., Plainview, NY, USA. P25 powder had a primary particle size of 40 μm, a specific surface area of 50 ± 1.5 m^2/g, and its crystalline mode was 20% rutile and 80% anatase type. Titaniumtetraisopropoxide (TIP), neodymium(III)acetylacetonate, palladium(II) acetylacetonate, iron(III)acetylacetonate, hexachloroplatinium(IV), and silica gel (Davisil^{TM}, 250-400 μm) were purchased from the Aldrich chemical Co (Milwaukee, WI.,USA). All chemicals were analytical grade and used without further purification. Deionized and double distilled water was used throughout this study. The pH of solutions was adjusted by NaOH or $HClO_4$ solution.

Preparation of transition metal doped TiO_2 thin films. The hot-wall low-pressure reactor setup is illustrated in Figure 1. The temperature profiles of the hot-wall CVD reactor were fitted with a sole function in distance with the temperature of the setting point a parameter. The central zone of the reactor (50 cm long) showed an almost constant temperature with variations of ± 5.0 K.

The precursors, titanium(IV)tetraisoproxide and neodymium (III) acetylacetonate were placed in an evaporator and graphite boat, respectively, and placed very close to the reactor entrance. The co-deposition of neodymium(III) and titanium(IV) dioxide were carried out at 80 Pa and 873 K at different TM/Ti ratios by varying the evaporation temperature of precursors (TIP 323-350 K, transition metal acetylacetonate 483-553 K). In both cases, argon was used as the carrier gas with a flow rate of 50 cm/sec, and at the reactor entrance, the additional flux of 10 cm/sec of oxygen was added.

Thin film characterization. Structure characterization of the TiO_2 doped and undoped was done by X-ray diffractometer (XRD; Rigaku D-Max B), equipped with a graphite crystal monochromater. The transition element concentrations on the surface of the TiO_2/support were measured with an X-ray photoelectron spectroscope (XPS Model ESCA 750), using a Al K_α exiting radiations. The observation of surface morphology and average grain size and distribution was performed with an AMRAY 1810 scanning electron microscope (SEM).

Photoreactor and light source. A bench-scale photoreactor system, as shown in Figure 2, consisted of a cylindrical pyrex-glass cell, 20 cm in diameter and 30 cm high inside-coated with mirror. And the UV lamp having the resource of 100 W Hg 1amp (Ace Glass Inc.) was immersed into the solution with air cooling jacket.

The photocatalytic reactor for the continuous flow experiment was constructed in series with four 30 cm-long quartz

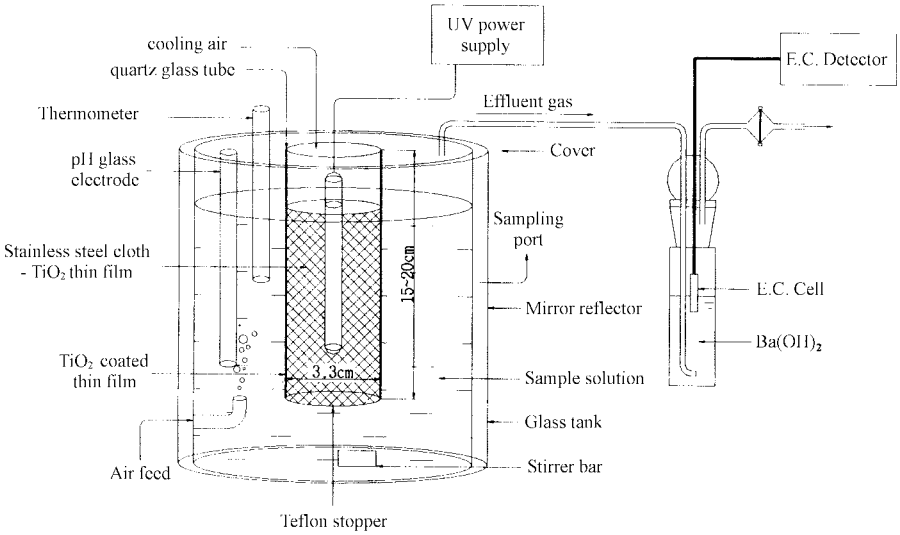

Figure 2. Schematic diagram of photocatalytic reactor for batch experiment.

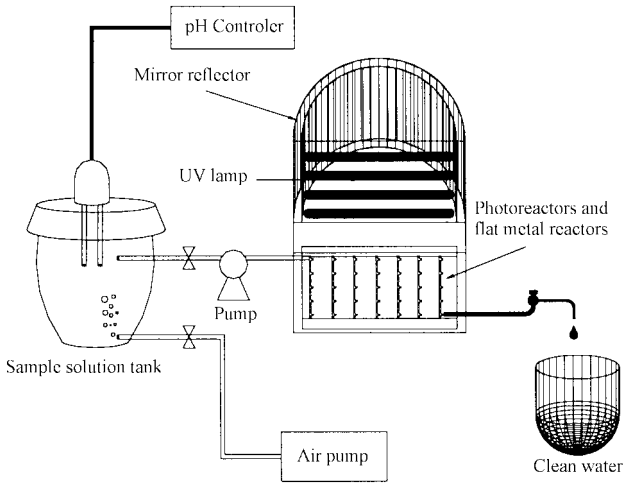

Figure 3. Schematic diagram of the continuous flow experiment setup used for screening photocartalytic/reactor option.

glass tubes (inside diameter = 3.3 cm) coated with the TiO_2 thin films inside the tube. As shown in Figure 3, ports of T shape of polytetrafluoroethylene (PTFE, Teflon) were constructed along the reactor to collect analytical samples at given intervals of illumination.

Up to 10 reactors, 5.0 cm apart as shown in Figure 3, were mounted in front of a flat metal plate reactor, and four 100-200 W UV lamps with a wavelength range of 300-400 nm, were mounted in the mirror reflector on the reactor. The distance from the photoreactors to the UV lamp was 10 cm. These reactors were operated in parallel so various TiO_2 thin film-capsules could be compared with one another under identical conditions. As shown in the flat metal reactor of Figure 3, the photocatalytic reactor A type for the continuous flow experiment was constructed in series of four 30 cm-long quartz glass tubes(inside diameter = 3.3 cm) coated with TiO_2 thin films on the inside of the tube. And for type B, a stainless steel cloth capsules or silica-gel coated with TiO_2 thin films was inserted or loaded into each pure quartz glass tube.

Procedure and analysis. Aqueous solution of the sample (usually 1000 mL) and the thin films (TiO_2/support, MO-TiO_2/support) were placed in a photoreactor cell. Before irradiation, the thin films were magnetically stirred in a dark place for *ca*. 30 min to establish an adsorption and desorption equilibrium between 2-CP and the thin film surface. At given intervals of illumination, a sample was collected in a test-tube or vial. Each sample solution was analyzed by HPLC (Hewlett-Packard series 1100 system) equipped with an UV detector (λmax = 210 nm) and column (2-CP: Eclipse XDB-C18 (50 mm × 0.5 mm), organic acids: Supelcogel C-610H (30 cm × 7.8 mm)). The eluent solvent was actonitirile; the buffer solution was H_3PO_4/NaH_2PO_4, pH = 3.0, and the eluent for organic acids was 1.0% H_3PO_4 .

The total organic carbon (TOC) of each sample solution was measured at constant irradiation time intervals, using a TOC analyzer (Tekmamar-Dohrmann, DC-190). The Cl^- ion was analyzed by an ion chromatograph (Dionex Bio LC Chromatography) equipped with an electrochemical detector and a Dionex PAX-100 metal-free anion column (25 cm length, 4.6 mm inside diameter). The eluent solution was a mixture of 80% H_2O, 10% acetonitrile and 10% 191 mM NaOH, and the flow rate was 1 mL/min; the injection loop was 50 μL in volume.

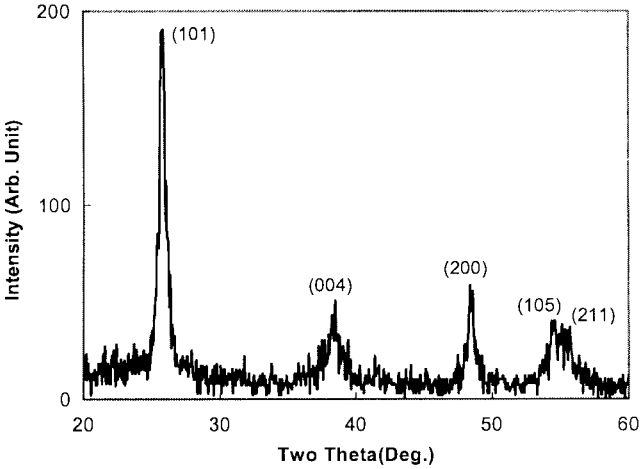

Figure 4. XRD patterns for the TiO_2 thin film doped with Nd(III) on SS.

Results and Discussion

Figure 4 is an XRD patterns for TiO_2 thin film doped with Nd(III) on SS.

The locations of (101), (004), (200), (105) and (211) diffraction peaks show that the film is a polycrystalline structure TiO_2 stoichiometry with an antase type, which is of a tetragonal Bravais lattice. The thin films also show a slight (101) preferred orientation. The full width at half maximum (FWHM) was used to calculate the grain size of the film, using Scherrers formula[25] from which the average value of the grain size was approximately 100 nm. TiO_2 in anatase form is believed to be the most efficient photocatalyst during the chemical reaction.[26-27] In addition to the diffraction peaks

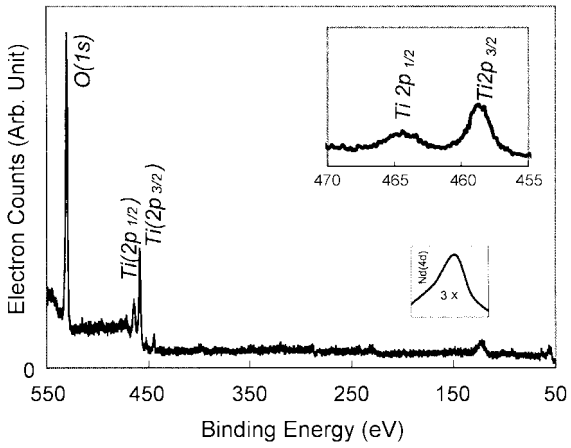

Figure 5. XPS patterns for the TiO_2 thin film doped with Nd(III) on SS.

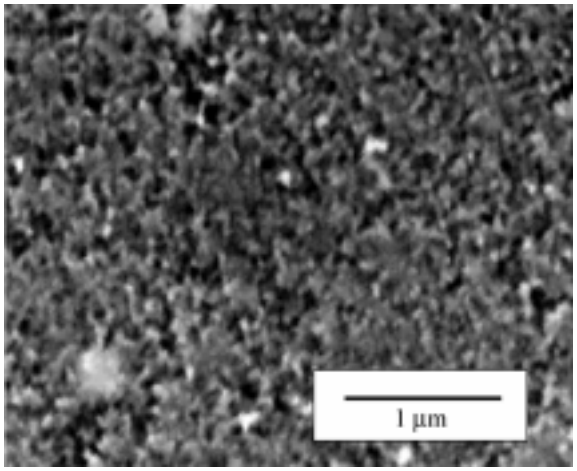

Figure 6. SEM picture of the TiO_2 thin film doped with Nd(III) on SS.

for the anatase, there were no extra detectable peaks for the TiO_2 rutile structure. Also, no Nd diffraction peak was available from the XRD result. This suggests that no separated phase appeared during the doping process.

Figure 5 shows representatively the results of the XPS survey for TiO_2 thin film doped with Nd(III) on SS. The insert in Figure 5 shows representatively the XPS patterns of the thin film.

Only peaks associated with Ti, O, and Nd were observable. Nd concentration was measured at 1.0 wt %, which is a relatively stable value achieved at steady state of the film after the ion etching. Besides the oxygen peak, there exist two Ti peaks, Ti ($2P_{3/2}$) and Ti($2P_{1/2}$), which are located at 458.4 eV and 464.1 eV, respectively. This resulted from different atomic binding environments of Ti in the film. And the 5.7 eV binding energy shift between them indicates the formation of TiO_2.[28]

The surface morphology of the thin film was examined by SEM. Figure 6 is the SEM picture for the 10000X magnified TiO_2 doped with Nd(III) on the surface of SS.

The light dots are the nano-dimensional TiO_2 grains. It is clear from Figure 6 that the surface of the film is very rough and most of the crystallites are regularly distributed. The catalyst is one of the main practical applications of TiO_2 in our experiment. Therefore, how to enhance the efficiency of the TiO_2 catalyst was critical. The different dopants can have different effects on the changes of catalyst efficiency, which we will discuss later here. And for the TiO_2 doped with the metal and substrate, such as stainless steel cloth, the efficiency was largely determined by the total area of the TiO_2 crystallites. Moreover, most of the contribution for the area increase was from the crystallite surface. In this sample, the nanometer size of grains provided a large surface area, which guarantees activity improvement. This uniformity of the distribution and size of TiO_2 mono-crystallite dose provides large surface area and enhances the activity of photocatalysts.

The results of the degradation of 2-CP, using the TiO_2 thin films doped with four transition metals, doped or pure

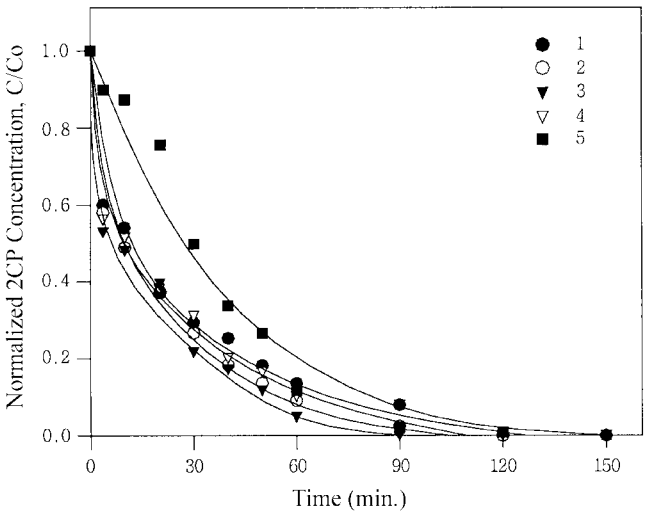

Figure 7. Comparison of 2-CP photodegradation by 1.0% TiO_2 thin films doped with four different transition metal on outside of QGT (40.08π cm^3), and by TiO_2-QGT thin film. [TiO_2-QGT thin films doped with: 1: Pd(II), 2: Pt(IV), 3: Nd(III) and 4: Fe(III), and (5) TiO_2-QGT thin film]

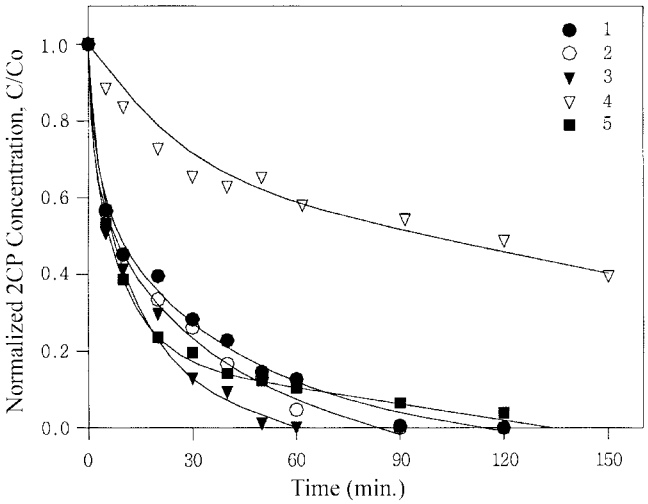

Figure 8. Comparison of 2-CP photodegradation by 1.0%wt TiO_2 thin films doped with four different transition metal on SS(37 μm, 40π cm^3), and by 1.0%wt TiO_2-SS thin film. [TiO_2-SS thin films doped with: 1: Pd(II), 2: Pt(IV), 3: Nd(III), 4: Fe(III), and 5: TiO_2-SS thin film.]

titanium dioxide thin films coated on supports, such as silica gel, quartz glass tube and stainless steel cloth, are presented in Figure 7 and Figure 8, in the batch experimental system of Figure 2, and in Figure 10, Figure 11 and Figure 12, in the continuous flow system of Figure 3, respectively.

Figure 7 and Figure 8 show the decrease in concentration as a function of irradiation time, and the transition metal-TiO_2 thin films coated on the supports, such as quartz glass tube and stainless steel cloth, exhibited a higher 2-CP destruction rate than the same supports coated with pure TiO_2 thin film prepared at identical experimental conditions.

Also four photocatalytic efficiencies of the four transition metals-TiO_2 thin films coated on the surface of three dif-

ferent supports have been compared with P25 powder. These results exhibited the activities of the photodegradation for 2-CP compared in Figure 7 and Figure 8. The results in Figure 7 and Figure 8 exhibited that activities of the photodegradation for 2-CP have been enhanced in the order of Nd(III) > Pt(IV) > Pd(II) > Fe(III) as a doping metal of TiO_2 thin film ,and SS > QGT as a support. Notably, 99% of 2-CP was destroyed within 60 min when neodymiumize TiO_2 thin film coated on the surface of SS was used as a photocatalyst.

The co-precipitation of metals onto the TiO_2 surface was one process employed to improve its photocatalytic efficiency.

The binding energy of the 4d electron at 122.0 eV indicates that the Nd(III) is in the metallic state since O is absent in the reaction system. The main photoreaction in this system is as follows:

$$TiO_2 + h\upsilon \rightarrow e^-(cb) + h^+(VB) \quad (1)$$

Where e^-(cb) and h^+(vb) donate the excited electrons in the conduction band and the holes in the valance band are of TiO_2 anatase type.

$$Nd^{3+} + 3e^- \rightarrow Nd \quad (2)$$

Assuming that the photodeposition of Nd(III) proceeds according to the Langmuir-Hinshewood (L-H) mechanism, *i.e.*, absorbed Nd^{3+} is reduced by e^- (CB) on the surface of TiO_2, one can write that rate equation as

$$\ln(\omega_1-\omega)/\omega = \kappa t \quad (3)$$

where ω and ω_1 are the weights of Nd deposited after the photoreduction time of t and infinity, respectively.

Figure 9 is the plot of $\ln(\omega_1-\omega)/\omega$ as a function of *t*. The value of $\ln(\omega_1-\omega)/\omega$ is proportional to *t*.

This finding suggests that the reaction occurs *via* the L-H mechanism and the quantity of Nd(III) loaded can be controlled by *t*. It must also be taken into consideration that the reduction in the flat band potential of TiO_2 with decreasing pH of solution decreases the rate of the reaction.[29]

Therefore, the photocatalytic efficiency of TiO_2 increases

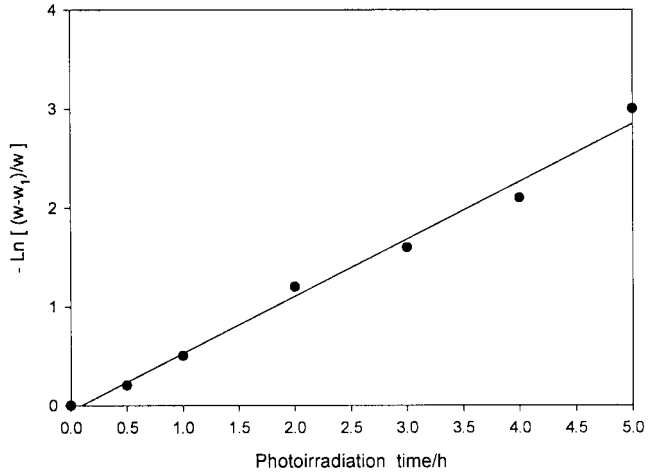

Figure 9. The plot of $-\mathrm{Ln}[(\omega_t-\omega)/\omega]$ as function of *t* on the dependence of the deposited amount of Nd-TiO_2-SS/UV system.

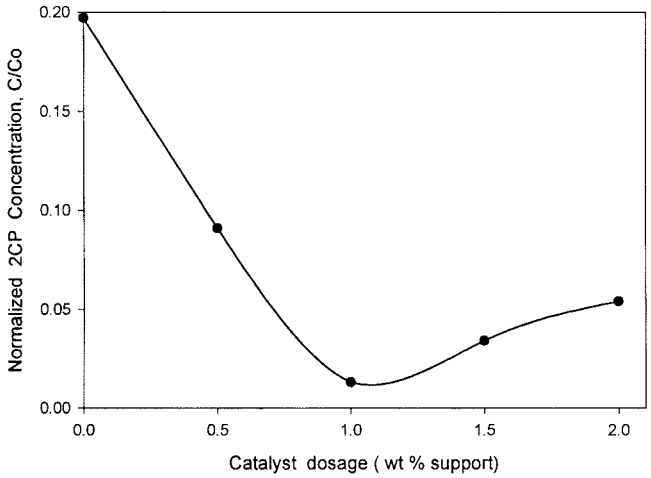

Figure 10. 2-CP photodegradation by capsule dosages of Nd-TiO_2-SS(37 μm, 40.08π cm^3) thin film.

with the presence of an electron acceptor, such as oxygen molecules or transition metals (M^{n+}), such as Nd(III), Pt(IV), and Pd(II), because the recombination of electron/hole pairs can be lessen.

The actual doping concentration of the transition metal ions in TiO_2 is related to the ionic radii. The ionic radii of these metal ions (1.1 Å) were much larger than that of Ti^{4+} (0.60 Å), thus, neodymium ions could not easily enter the lattice of TiO_2 because the concentration of metal ions entering the lattice of TiO_2 was very small.

For Nd(III), Pt(IV), and Pd(II) ion doped on the surface of TiO_2 thin films, the solid vapor formed by the CVD method contained a very low content of metal ions**;** part of metal ions was adsorbed on the surface of TiO_2 thin films. However, the low doping of metal ions in TiO_2 may favor the separation of electrons and holes, prolong the life time of carriers, reduce the recombination of electrons and holes, and finally promote the photodegradation of 2-CP enhancement.

The adhesion of TiO_2 on its support was of good quality with the exception of silica gel since no detachment of TiO_2 could be observed during several photocatalytic tests. This adhesion was induced by heating the sample at the range of 550-650 °C in vacuum state. As a consequence, there was a migration of some cations (Na^+, Si^{4+}) from the support, such as silica gel, to the TiO_2 layer.[30] These ions dissolved in the lattice of TiO_2 thin films constitute the recombination of hole-electron centers and hence inhibitors. This could explain why silica gel decreases the photocatalytic activity of TiO_2 thin films. However, the SS and quartz glass tube, which by contrast are much more inert and stable under heating, allow the preparation of more deposited thin films. Also the photocatalytic efficiency of TiO_2 thin film doped with Fe(III) on the surface of SS and QGT has been decreased much more than 1.0 gL^{-1} P25 powder.[31a,b] For Fe^{3+}-doped films, although the nature of Fe^{3+} centered in anatase TiO_2 thin film is unknown, Gratzel and Howe[32] suggest that the Fe^{3+} ions are substitutionally located in Ti^{4+} lattice sites. The substitutional procedure is expected to

influence the placement of the Fe^{3+} ions within the TiO_2 lattice. It is possible that the low reactivity of Fe^{3+}-doped films coated on the surface of SS may have been due to the fact that Fe^{3+} ions acted as charge carrier recombination site.

Also found is that the doped or non-doped thin films coated on the surface of SS or quartz glass tube retained a constant photocatalytic activity when reused after mere rinsing of the thin films in deionized water. This indicates that deposited TiO_2 thin films with Nd(III), Pt(IV), or Pd(II) are not deactivated during the photoreaction either by inhibition or loosening or poisoning of the photocatalyst. Thus, these thin films can be re-utilized in subsequent runs.

The neodymiumize TiO_2 thin film coated on the surface of SS was evaluated with catalyst dosages of 0.5, 1.0, 1.5 and 2.0 wt. %.

Figure 10 shows the changes of 2-CP concentration at the 60 minute sample ports of reactors for the various catalyst dosages.

Clearly, the optimal catalyst dosage was 1.0 wt. %, as a shown in Figure 10. These results suggest that the higher UV light transparent support required a lower weight percent of the photocatalyst on the support (SS) than the lower UV transparent support to achieve the best degradation. This result coincides with the catalyst dosage that has photo-decomposed trichloroethylene using Pt-TiO_2 thin film coated on the silica-gel.[31b,33]

Figure 11 shows the effect of the influence of hydraulic loading on the Nd-TiO_2-SS thin films.

The rates of 2-CP photodegradation for the Nd-TiO_2-SS thin film were increased in the order of flow-rate. However, good degradation is observed over a range of 18-27 m/h. The 85% 2-CP is degraded by a 120 cm reactor length, having four capsule of the Nd-TiO_2-SS thin film at a hydraulic loading of 18 m/hour.

Therefore, the effective factor of 2-CP degradation, using the Nd-TiO_2-SS thin film, can be 2.64×10^{-1} $mgL^{-1}cm^{-3}$ when mass transfer does not limit the degradation-rate.[35] The effective factor did not include the enhancement by mass transfer due to OH-2CP reaction in the diffusion boundary layer surrounding the catalyst. If the enhancement is considered, the length of the reactor may be expected to be shorter and the effective factor to increase per capsule of the catalysts.

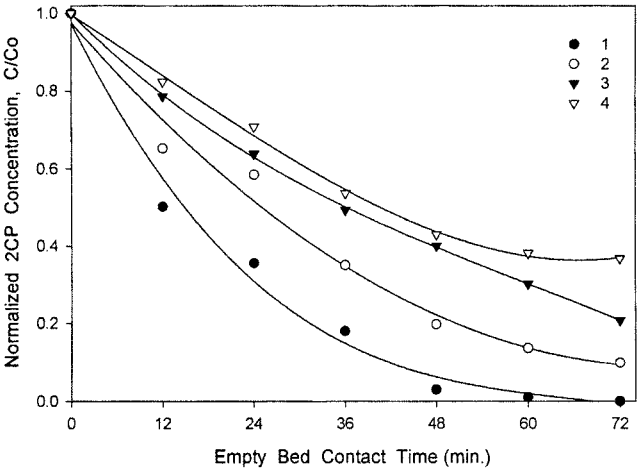

Figure 12. Comparison of 2-CP photodegradation by 1.0 wt% Nd-TiO_2-SS, TiO_2-SS, and Nd-TiO_2-SG thin films, and for P25 suspended solution. [1: Nd-TiO_2-SS(37 μm, 40.08π cm^3) 2: TiO_2-SS 3: Nd-TiO_2-SG(10.0 gL^{-1}), and 4: 1.0 g/L P25 suspended solution.]

The four photocatalytic efficiencies of the neodymumize and pure TiO_2 thin films coated on both surfaces of the stainless steel cloth capsule have been compared with those of P25 powder in the Figure 12.

The effluent concentration of 25.0 mg/L 2-CP adjusted at pH 11.0 was used at hydraulic loading of 18 m/h for each photocatalyst. The experiment was illuminated by 200 W UV-lamp under air cooling and saturation conditions. The results of Figure 13 exhibited that the activities of each capsule were enhanced in the order of Nd-TiO_2-SS thin film > TiO_2-SS > P25 powder > TiO_2-SG thin film.

About 99% of 2-CP was destroyed within 60 minutes as a function of empty bed contact time in the case of the Nd-

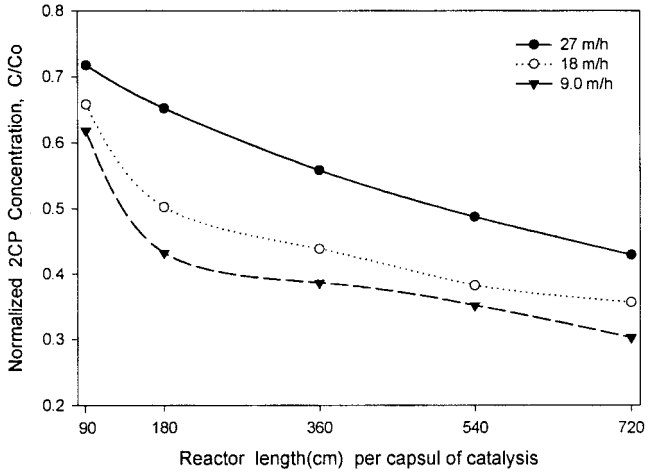

Figure 11. Influence of hydraulic loading for 2-CP photo-degradation by 1.0 wt % Nd-TiO_2-SS(37 μm, 4.08π cm^3) thin film.

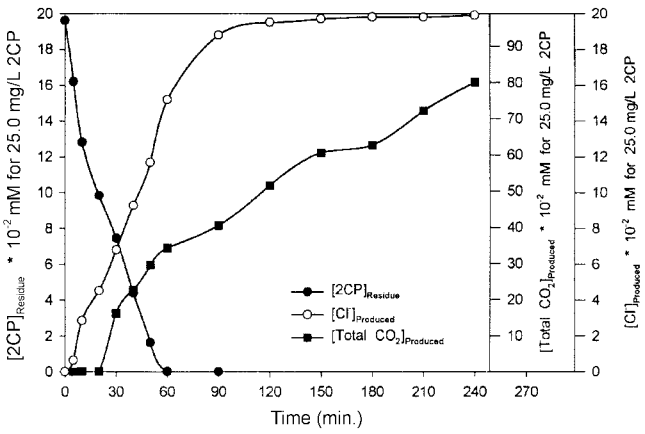

Figure 13. Changes of [2-CP], $[Cl^-]$, and $[\Sigma CO_2]$ in the process of 2-CP photodegradation ,using 1.0%wt Nd-TiO_2-SS(37 μm, 40π cm^3) thin film.

TiO_2-SS thin film.

Figure 13 shows the normalized 2-CP degradation, the chloride ion (Cl^-, and total carbon dioxide ($[CO_2]_g + [HCO_3^-]$) production as a function of illumination time when the Nd-TiO_2-SS thin film has been used as photcatalysis.

The causes for 2-CP disappearance include formation of intermediates or byproducts, adsorption onto the catalysis/ support. Although the chloride ion emergence lags behind the 2-CP disappearance, all of the chlorinated intermediates were destroyed within 90 minutes in the batch experiment. The formation of chloride ions is slower than the degradation of 2-CP. For example, about 85% of 2-CP was degraded but 75% of chloride ions were observed after 40 minutes of photooxidation, using the Nd-TiO_2-SS/UV system, and although 2-CP has been perfectly degraded, the chloride ion production was observed up to about 90 minutes in this system. The difference in the 2-CP degradation and dechlorination suggests the formation of some chlorinated intermediate products. This agrees with the above analysis of reaction products, where chlorinated intermediates have been determined as the major reaction products.

Also total carbon dioxide emergence were detected behind the 2-CP, and chlorinated intermediates were perfectly disappeared. The rate of the evolution of total carbon dioxide is much slower than the rate of the formation of chloride ions, which suggests the formation of non-chlorinated products. For example, although 100% of chlorinated intermediates were degraded, the products of total carbon dioxide are only about 40% at 120 minutes of photooxidation. However, after 210 minutes of illumination of the sample under experimental conditions (Figure 13), about 61% of total carbon dioxide was released from the sample.

This suggests that some major organic acids such as tartaric, glyoxalic, succinic, malic, oxalic, acetic and formic acid were part of the reaction products[34-35] produced in the present study. This indicates that the photocatalytic oxidation process with TiO_2-SS thin films prepared by CVD methods is effective in completely mineralizing 2-CP to carbon dioxide and chloride ions within 300 minutes at these experimental conditions. However, it is interesting to note that UV photolysis alone yields only about 2% carbon dioxide, and photolysis by Nd-TiO_2-SS thin film/UV system yields about 98% carbon dioxide under similar experimental conditions.

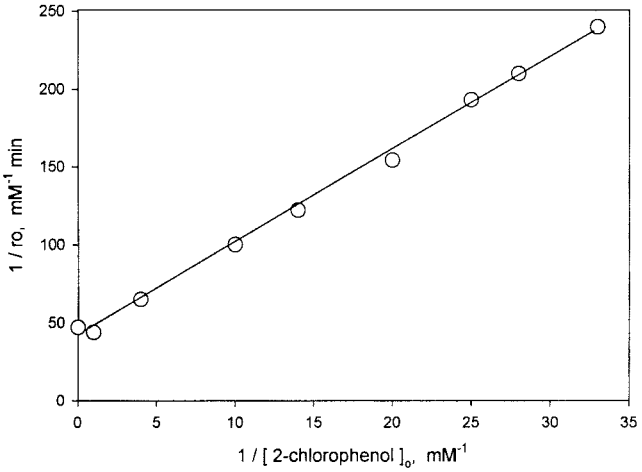

Figure 14. The reciprocals of the initial rates *vs*. the reciprocals of the 2-CP concentrations.

Figure 14 gives the initial rates, r_0 *vs*. the initial 2-chlorophenol concentration, $[2CP]_0$ in the process of photooxidation, using Nd-TiO_2-SS thin films prepared by the CVD method.

The initial rates under batch experiments are proportional to the initial 2-CP concentrations. When the reciprocals of the initial rates are plotted against the reciprocals of the initial 2-CP concentrations, using the Langmuir-Hinshelwood equation (equation 4),[34] a linear relationship is obtained with $r^2 = 0.99$.

$$1/r_0 = 1/k + 1/kK[2CP]_0 \quad (4)$$

Results from regression analysis for the Nd-TiO_2-SS thin film show that the rate constant (k) is 3.52×10^{-3} mM min^{-1} and the adsorption coefficient (K) is 6.43 mM^{-1}. The good fit with the Langmuir-Hinshelwood relationship indicates that the degradation of 2-CP is likely to occur at the surface of Nd-TiO_2-SS thin films in a photocatalytic oxidation process.

Tables 1 and 2 give the pseudo first order rate constants (k, mole min^{-1}) and half period ($t_{1/2}$, mole min^{-1}) for 2-CP degradation (k_{2CP}), chloride ion production (k_{cl}) and total

Table 1. Summary of kinetic results (k) of photodegradation of 2-CP

	Nd-TiO_2-SS	Nd-TiO_2-QGT	Pt-TiO_2-SS	Pd-TiO_2-SS	Fe-TiO_2-SS	P25	UV-alone	TiO_2-SS
2CP	3.52×10^{3}	2.94×10^{-3}	3.22×10^{-3}	2.92×10^{-3}	1.27×10^{-3}	2.28×10^{-3}	1.35×10^{-4}	2.54×10^{-3}
Cl^-	1.74×10^{-3}	1.49×10^{-3}	1.58×10^{-3}	1.50×10^{-3}	7.02×10^{-4}	1.16×10^{-3}	1.26×10^{-4}	1.31×10^{-3}
ΣCO_2	7.62×10^{-4}	6.01×10^{-4}	7.13×10^{-4}	6.53×10^{-4}	1.81×10^{-5}	5.18×10^{-4}	$> 10^{-6}$	5.38×10^{-4}

Table 2. Summary of half period ($t_{1/2}$) of photodegradation of 2-CP

	Nd-TiO_2-SS	Nd-TiO_2-QGT	Pt-TiO_2-SS	Pd-TiO_2-SS	Fe-TiO_2-SS	P25	UV-alone	TiO_2-SS
2CP	20	24	21	23	158	38	456	28
Cl^-	35	43	39	42	280	61	500	52
ΣCO_2	126	140	130	135	$>10^3$	163	–	145

*TiO_2-SS (CVD, 40ϕ cm^3, 37 μm), Nd(III), Pt(IV), Pd(II), Fe(III), TiO_2-QGT (40.84 ϕ cm^3). P25 (1.0 gL^{-1}) , and UV-alone (100W)

Table 3. Major mass spectra and HPLC data* of photodegradation of 2-CP

PT (min)	intermediate	R.T. (min)	m/z	Quantity (%)
0-60	2-chlorophenol	12.5	128	82.5
10-60	catechol	10.2	110	0.4
5-120	2-chlorocatechol	14.8	144	6.8
5-70	4-chlororesocinol	15.2	144	0.6
5-120	chlorohydroquinone	15.6*	144	12.1
5-210	glyoxylic acid	6.92*	74.0	46.4
40-210	succinic acid	9.03*	100	16.2
5-150	maleic acid	5.12*	116	0.3
5-40	acetic acid	10.1*	103	6.6
5-150	oxalic acid	8.61*	90.5	3.2

*Eluent: 1.0% H_3PO_4 (f = 0.1 mL min^{-1}) for organic acids and 2-chlorocathechol. PT; Photooxidation time (min). RT; Retention time (min)

carbon dioxide generation (k_{CO2}) in the presence of UV alone and photocatalyst (Nd-TiO_2-SS, Nd-TiO_2-QGT, Pt-TiO_2-SS, Pd-TiO_2-SS and Fe-TiO_2-SS thin film, and P25 powder) plus UV, respectively ,under batch experiment .

In the presence of UV alone, the 2-CP photodegradation rate is almost identical to the rates of formation of chloride ions; this implies that the initial step of the direct photolysis reaction may mainly be the dechlorination. However, when the TiO_2 thin films or pure TiO_2 are added to the same system, the dechlorination rates constants are about half that of the 2-CP degradation, which indicates that reactions other than dechlorination occur. Apparently, the non-dechlorination reactions occurred during the photocatalytic oxidation reaction of 2-CP, yielding chlorinated intermediates. And the reaction kinetics of the photooxidation in this experiment have been decreased in accordance with the increase in reaction time due to an increase in the concentration of bicarbonate ion in the reaction solution. Bicarbonate ion (HCO_3^-) is known as OH radical scavenger. In the present study, bicarbonate ion was found to be the primary inhibitor of 2-CP destruction.

Five major organic acids have been ascertained as the ring cleavage products of oxidation of 2-CP by the ·OH radical (Table 3).

These radicals are generated through HHQ and then 1,2, 4,5-tetrahydroxybenzene (TeHB).[34-35] Further oxidation of TeHB produced 3,4-dihyroxy-2-4-hexadiene-1-6-dicarboxylic acid, which was further oxidized to glyoxalic, tartalic, succinic, oxalic malic, and acetic acids. The final step of photooxidation is the conversion of organic acids to carbon dioxide.

Conclusion

From the XRD patterns and XPS spectrum of TiO_2 thin films prepared by CVD and sol-gel methods, The confirmation was made that the films were polycrystalline structure of TiO_2 anatase type, which is believed to be the most efficient photocatalyst. The average grain size obtained from CVD is approximately 100 nm.

The photocatalytic efficiency of TiO_2 is dramatically enhanced by thin films supported on various matrixes and prepared by different methods, including CVD (400-550 °C) and Sol-gel (600-650 °C). A relation between the photochemical behavior of TiO_2 coating and its structure can be established with respect to the effect of heat-treatment temperature.

The increase in photocatalytic activity above 400 resulted from the formation of crystalline TiO_2. The sol-gel method, however, formed amorphous TiO_2. The photocatalytic efficiency of the TiO_2 thin films coated by the CVD method have exhibited better photocatalytic activity than the sol-gel methods. Comparing to SS, QRT, and SG, shows that SG is not a good support for TiO_2 thin film, because the Na^+ or Si^{4+} ion dissolved in the lattice of TiO_2-SG thin films decreases the photoefficiency of TiO_2.

Transition metals such as Pd(II), Pt(IV), Nd(III) and Fe(III) were doped onto TiO_2 thin film by the MOCVD method. The results show that activities of the photodegradation for 2-CP have been enhanced in the order of Nd(III) > Pt(IV) > Pd(II) > Fe(III) as a doping metal of TiO_2 thin film. Among all supporting materials studied, SS(37 μm) appears to be the best support, both for batch and continuous flow experiments. An optimal amount of doping material at 1.0%(w/w) of TiO_2 -substrate thin film gives the best photodegradation of 2-CP.

Photocatalytic oxidation by-products generated in the process of the degradation of 2-CP are mainly organic carboxylic acids. In the present study, an easy and accurate analytical method was established to monitor the organic acid concentration. This procedure is also applicable to analysis of photocatalytic oxidation of various organic contaminants.

References

1. Hoffman, M. R.; Martin, S. T.; Choi, W.; Bahnenann, D. W. *Chem. Rev.* **1995**, *95*, 69.
2. Ollis, D. F.; Al-Ekabi, H. *Photocatalytic Purification and Treatment of Water and Air*; Elsevier: Amsterdam, 1993.
3. *Proceedings of NATO Advanced Research Workshop on Homogeneous and Heterogeneous Photocatalysis*; Maratea: Italy, 1995; p 721.
4. Fox, M. A.; Dulay, M. T. *Chem. Rev.* **1993**, *93*, 341.
5. Suri, R. P. S.; Crittenden, J. C.; Fellow, P. E.; Hand, D. W. *Environ. Eng.* **1999**, *125*, 897.
6. Peill, N. J.; Hoffman, M. R. *Environ. Sci. Technol*. **1996**, *30*, 2809.
7. Litter, M. L.; Navio, J. A. *J. Photochem. Photobiol. A* **1994**, *98*, 183.
8. Murata, Y.; Fukuda, S.; Ishikikawa, S.; Yokoyama, S. *Solar Energy Materials and Solar Cells* **2000**, *62*, 157.
9. Wang, Y.; Cheng, H.; Hao, Y.; Ma, J.; Li, W.; Cai, S. *J. Mater. Sci*. **1999**, *34*, 3721.
10. Bard, A. J.; Bernhard, K. *US Patent* **1981**, *4*, 303, 486.
11. Fernandez, A.; Lassaletta, G.; Jimenez, V. M.; Justo, A.; Gonzales, A. R.; Herrmann, J. M.; Tahiri, H.; Ait-Ichou, Y. *App. Cat. B: Environ*. **1995**, *7*, 49.
12. Roberto, J. C.; Walter, A. Z.; Anderson, A. *J. Environ. Eng*. **1999**, 906.
13. Byme, J. A.; Eggins, B. R.; Brown, N. M. D.; McKinney,

B.; Rouse, M. *App. Cat. B: Environ.* **1998**, *17*, 25.
14. Zakharenko, V. S. *Catalysis Today* **1997**, *39*, 243.
15. Xingtao, G.; Israel, E. W. *Catalysis Today* **1999**, *51*, 233.
16. Leyva, E.; Moctezuma, E.; Ruiz, M. G.; Torres-martinez, L. *Catalysis Today* **1998**, *40*, 367.
17. Ha, H. Y.; Anderson, M. A. *Environ. Eng*. **1996**, 217.
18. (a) Zorn, M. E.; Tompkins, D. T.; Zeltner, W. A.; Anderson, M. A. *Applied. Catalysis B: Environ*. **1999**, *23*, 1. (b) Ranjit, K. T.; Willner, I.; Bossmann, S.; Braun, A. *J. Phys. Chem*. *B* **1998**, *102*, 9397.
19. Ding, Z.; Hu, X.; Lu, G. Q.; Yue, P. L.; Greenfield, P. F. *Langmuir* **2000**, *16*, 6216.
20. Navio, A. J.; Testa, J. J.; Djedjeian, P.; Padron, J. R.; Rodriguez, D.; Litter, M. I. *Applied Catalysis A: General* **1999**, *178*, 191.
21. Guerin, D.; Saha, S. I. *J. Vac. Sci. Technol. A* **1997**, *15*, 712.
22. Battiston, G. A.; Gerbasi, R.; Porchia, M.; Gasparotto, A. *Chem. Vap. Deposition* **1999**, *5*, 1.
23. Krumdieck, J. S.; Raj, R. *J. Am. Ceram. Soc.* **1999**, *82*, 1605.
24. Chemseddine, A.; Moriz, T. *Eur. J. Inorg. Chem.* **1999**, *202*, 235.
25. Spurr, A. R.; Myers, M. *Anal. Chem.* **1957**, *29*, 760.
26. Sclafani, A.; Palmisano, E.; Davi, E. *Photochem. Photobiol. A: Chem.* **1991**, *56*, 113.
27. Vidal, A.; Herrero, J.; Romero, M.; Sanchez, B.; Sanchez, M. *J. Photochem. Photobiol. A: Chem.* **1994**, *79*, 213.
28. *Handbook of X-ray Photoelectron Spectroscopy*; Wagner, C. D., Ed.; Perkin Elmer: Minnesota, USA, 1979.
29. Toda, H.; Honda, H. *J. Electrochem. Soc*. **1995**, *142*, 3438.
30. Fernandez, A.; Lassaletta, G.; Jimenez, V. M.; Justo, A.; Gonalez-Elipe, A.; Herrmann, J.-M.; Tahiri, H.; Ait-Ichou, Y. *Applied Cat. B: Environ.* **1995**, *7*, 49.
31. (a) Jose, A. N.; Juan, J. T.; Pablo, D.; Javier, R. P.; Dina, R.; Marta, I. L. *Applied Catlysis A: General* **1999**, *178*, 191. (b) Sawunyama, P.; Yasumori, A.; Okada, K. *Material Res. Bulletin* **1998**, *33*, 795.
32. Gratzel, M.; Howe, R. F. *J. Phys. Chem.* **1990**, *94*, 2556.
33. Yin, Z.; John, C. C.; David, W. H.; David, L. P. *Environ. Sci. Technol.* **1994**, *28*, 435.
34. Tseng, J. M.; Huang, C. P. *Wat. Sci. Tech*. **1991**, *23*, 377.
35. Jung, O. J.; Sung, M.; Huang, C. P. *Chemosphere* **2001**, inpress.